Eur. Phys. J. A (2023) 59:44
https://doi.org/10.1140/epja/s10050-023-00950-8

THE EUROPEAN PHYSICAL JOURNAL A

Regular Article - Experimental Physics

# In-beam $\gamma$-ray spectroscopy of $^{94}$Ag

**X. Pereira-López[1,2,a], M. A. Bentley[1,b], R. Wadsworth[1], P. Ruotsalainen[3], S. M. Lenzi[4,5], U. Forsberg[1,6], K. Auranen[3], A. Blazhev[7], B. Cederwall[8], T. Grahn[3], P. Greenlees[3], A. Illana[3], D. G. Jenkins[1], R. Julin[3], H. Jutila[3], S. Juutinen[3], X. Liu[8], R. Llewelyn[1], M. Luoma[3], K. Moschner[7], C. Müller-Gatermann[7,9], B. S. Nara Singh[10,11], F. Nowacki[12], J. Ojala[3], J. Pakarinen[3], P. Papadakis[13], P. Rahkila[3], J. Romero[3,14], M. Sandzelius[3], J. Sarén[3], H. Tann[3,14], S. Uthayakumaar[1], J. Uusitalo[3], J. G. Vega-Romero[1], J. M. Vilhena[10], R. Yajzey[1,15], W. Zhang[1,8], G. Zimba[3]**

[1] School of Physics, Engineering and Technology, University of York, Heslington, York YO10 5DD, UK
[2] Center for Exotic Nuclear Studies, Institute for Basic Science (IBS), Daejeon 34126, Republic of Korea
[3] Department of Physics, University of Jyväskylä, P.O. Box 35, 40014 Jyvaskyla, Finland
[4] Dipartimento di Fisica e Astronomia "Galileo Galilei", Università di Padova, 35131 Padua, Italy
[5] INFN, Sezione di Padova, 35131 Padua, Italy
[6] Department of Physics, Lund University, 22100 Lund, Sweden
[7] Institute of Nuclear Physics, University of Cologne, 50937 Cologne, Germany
[8] Department of Physics, KTH-Royal Institute of Technology, 10691 Stockholm, Sweden
[9] Argonne National Laboratory, 9700 S Cass Av, Lemont 60439, USA
[10] School of Computing Engineering and Physical Sciences, University of the West of Scotland, Paisley PA12BE, UK
[11] School of Physics and Astronomy, Schuster Laboratory, Brunswick Street, Manchester M13 9PL, UK
[12] Université de Strasbourg, 67037 Strasbourg, France
[13] STFC Daresbury Laboratory, Daresbury, Warrington WA4 4AD, UK
[14] Department of Physics, Oliver Lodge Laboratory, University of Liverpool, Liverpool L69 7ZE, UK
[15] Department of Physics, Faculty of Science, Jazan University, 45142 Jazan, Saudi Arabia

Received: 20 December 2022 / Accepted: 9 February 2023

Communicated by Robert Janssens

**Abstract** A recoil-beta-tagging experiment has been performed to study the excited $T = 0$ and $T = 1$ states in the odd–odd $N = Z$ nucleus $^{94}$Ag, populated via the $^{40}$Ca($^{58}$Ni,1p3n)$^{94}$Ag reaction. The experiment was conducted using the MARA recoil separator and JUROGAM3 array at the Accelerator Laboratory of the University of Jyväskylä. Through correlating fast, high-energy beta decays at the MARA focal plane with prompt $\gamma$ rays emitted at the reaction target, a number of transitions between excited states in $^{94}$Ag have been identified. The timing characteristics of these transitions confirm that they fall within decay sequences that feed the short-lived $T = 1$ ground state of $^{94}$Ag. The transitions are proposed to proceed within and between the sets of states with $T = 0$ and $T = 1$. Possible correspondence between some of these transitions from analog states in $^{94}$Pd has been discussed, and shell-model calculations including multipole and monopole electromagnetic effects have been presented, in order to enable predictions of the decay patterns between the $T = 0$ and $T = 1$ states and to allow a theoretical set of Coulomb energy differences to be calculated for the $A = 94$ $T = 1$ analog states.

## 1 Introduction

The nuclei along the $N = Z$ line provide a unique opportunity to investigate one of the key underpinning concepts in nuclear physics: the exchange symmetry between neutrons and protons (isospin symmetry). In $N = Z$ systems protons and neutrons occupy the same orbitals, allowing for phenomena that are strongly influenced by the various types of neutron-proton interaction. In order to classify the different neutron-proton interactions, and different types of nuclear pairing correlations, we use the formal concept of isospin, originally introduced by Heisenberg [1] to account for the apparent charge independence of the nucleon-nucleon interaction. Like-nucleon pairing (neutron-neutron and proton-proton pairing), considered to be the dominant pairing correlation in nuclear structure, has isospin $T = 1$ and coupled angular momentum $J = 0$. However, in $N \sim Z$ systems two additional pairing types are possible. The first is the

[a] e-mail: xpereiralopez@ibs.re.kr (corresponding author)
[b] e-mail: michael.bentley@york.ac.uk (corresponding author)

Published online: 15 March 2023

$T = 1$ neutron-proton pairing – analogous to the $T = 1$ like-nucleon pairing – and $T = 0$, $J > 0$ pairing. The former type of np-pairing is common, and appears on an equal footing with the $T = 1$ nn- and pp-pairing. This type of pairing is especially obvious in odd–odd $N = Z$ systems (such as the $^{94}$Ag case being studied here) where a sequence of states with $T = 1$ is usually observed at, or near, the ground state, which has properties of a fully paired structure. These are the isobaric analog states of the $T = 1$ ground-state sequences of the neighbouring even–even isobars. The evidence for the second type of np-pairing ($T = 0$, $J > 0$) is, to date, much more elusive. This type of pairing is forbidden by the Pauli principle for like-nucleon pairs, and hence is expected to be significant only for nuclei on, or close to, the $N = Z$ line.

The heaviest accessible nuclei along the $N = Z$ line provide the optimal location for the existence of structures based on $T = 0$ np pairs, and these have been the focus of a number of different experimental studies (e.g. [2–4]). Despite the experimental efforts, convincing evidence for the $T = 0$ pairing mode still evades observation and hence it remains an open question whether the $T = 0$ pairs have significant relevance in the nuclear structure of these nuclei. Recently, however, properties of the rotational alignment of nucleons in the $N = Z$ nucleus $^{88}$Ru [3] have been interpreted in the context of the $T = 0$ np pairing. Of particular interest in these studies is the suggestion that spin-aligned np pairs dominate the wave function of the yrast sequence in $^{92}$Pd [2]. Subsequent theoretical studies [5–7] were devoted to probing the contribution of np pairs in other $N = Z$, $A > 90$ nuclei, such as $^{94}$Ag and $^{96}$Cd. These studies also indicate the potential for significant contributions from spin-aligned np pairs in the wave functions of the $T = 1$ states in odd–odd $N = Z$ nuclei, such as $^{94}$Ag.

The motivation for the current study was twofold. Firstly, the experiment sought to establish both the $T = 1$ and $T = 0$ excited states of the odd–odd $N = Z$ nucleus $^{94}$Ag. Several experimental studies have been focused on $^{94}$Ag [8–23]. However, current knowledge is limited to the $0^+$ ground state, with a half-life of 27(2) ms (weighted average of the results from [19] and [15]) and two isomeric states with tentative spin-parity assignments $(7^+)$ and $(21^+)$ [10], whose half-lives have been measured to be 0.50(1) s (weighted average from [19] and [16]) and 0.39(4) s [16], respectively. The $0^+$ state is assumed to be the $T = 1$ ground state – the analog of the $T = 1$ ground-states of even–even $^{94}$Pd and $^{94}$Cd. The short half-life of the $0^+$ ground-state in $^{94}$Ag indicates a superallowed $\beta$ decay between these $T = 1$ analog states. The isomers are $T = 0$ states, with the high-spin isomer located at $\sim$ 6.7 MeV [17] which was observed to decay through $\beta$, proton and $\beta$-delayed proton emission channels. It is interesting to note that the absolute separation in energy between the $T = 1$ and $T = 0$ structures in $^{94}$Ag has been predicted [6] to be dependent on the strength of the maximally aligned ($J = 9$) neutron-proton $g_{9/2}$ matrix element. Thus, the relative positions of these states may shed light on the importance of the spin-aligned np-pairing phenomenon [2] in this nucleus.

**Table 1** Beam energy, current and irradiation time for each of the beam settings. The same natural calcium target was used during the whole experiment

| Beam energy (MeV) | Beam current (pnA) | Irradiation time (h) |
|---|---|---|
| 157 | 2–4 | 20 |
| 167 | 2.5 | 116 |
| 177 | 1–2 | 44 |
| 183 | 1–3 | 63 |

The second motivation comes from examining the differences in excitation energy between the $T = 1$ states, if they can be established in $^{94}$Ag, and their analog states in even–even $^{94}$Pd. In the absence of isospin-breaking effects, the two sets of analog $T = 1$ states would be structurally identical. Naturally, the Coulomb force will break the degeneracy, although the underlying wave functions are expected to retain their isospin symmetry. A significant body of work has built up in recent years examining the difference in excitation energies between mirror pairs and complete $T = 1$ isobaric triplets – see, for example, references [12,24–38]. These studies, which have involved a shell-model interpretation, have shown that the electromagnetic effects within the shell-model cannot account alone for the energy differences, suggesting that other effective isospin-symmetry-breaking interactions are missing from the models – see [39–42]. An odd–odd $N = Z$ nucleus is the central ($T_z = 0$) member of a $T = 1$ isobaric triplet and, where excited states in all three members of the triplet have been established, Triplet Energy Differences (TED) are usually analysed [42] using all three sets of states. However, for nuclei above $A = 74$, the proton-rich members of the triplet are unknown, and the comparisons are restricted to differences between the odd–odd and even–even members with $T_z = 0, 1$ – called Coulomb energy differences (CED). CED are more complicated to model since they have contributions from both isovector and isotensor interactions (e.g. [12]) and, unlike TED, are sensitive to the details of the underlying configurations. These configurations are expected to be complex in the deformed $A \sim 70$ region and may not be well reproduced by the shell-model. No CED have been established to date in the $A = 90$ region, where the structure is better reproduced by accessible shell-model calculations.

In the present work, we have performed a recoil-$\beta$-tagging study of the odd–odd $N = Z$ nucleus $^{94}$Ag, located at the limits of nuclear binding for the $N = 47$ and $Z = 47$ isotonic and isotopic chains. We report here the first observed $\gamma$ ray transitions from states in $^{94}$Ag. The identified transi-

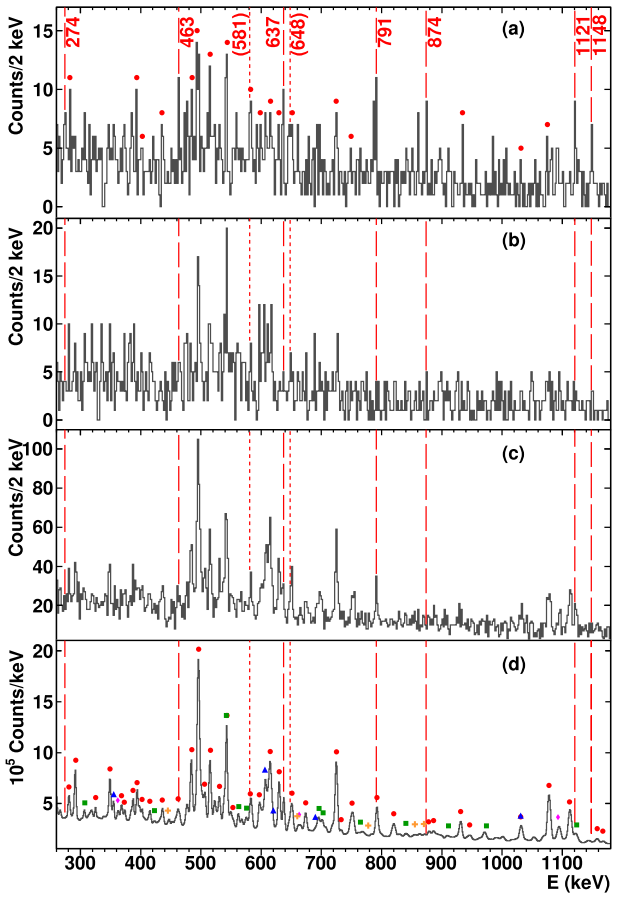


**Fig. 1** Doppler-corrected spectra for prompt $\gamma$ rays associated with $A = 94$ recoils observed in the focal plane decaying within **a** 60 ms or **b** between 120 and 180 ms from implantation in coincidence with a high-energy $\beta$-particle. Events in which two or more charged-particles were detected in the JYtube have been rejected. Panel **c** shows the same spectrum as **a** but where two or more charged-particles were detected in the JYTube. Panel **d** presents the prompt $\gamma$ rays measured with implantation of any $A = 94$ recoil. Highlighted in red dashed lines are shown the $^{94}$Ag transitions identified in **a** in this work. In **d**, symbols indicate observed known transitions of $^{94}$Ru (red circles), $^{94}$Rh (green squares), $^{94}$Tc (blue triangles), $^{94}$Mo (pink diamonds) and $^{90}$Mo (orange crosses) – see text for details

tions have been shown to be within decay paths that feed into the $T = 1$ ground-state, and some of the transitions may be associated with analog transitions between the $T = 1$ states in $^{94}$Pd. Shell-model calculations based on the JUN45 interaction [43] have been performed to extract CEDs. These are discussed with reference to some of the newly identified $\gamma$ ray transitions in $^{94}$Ag.

## 2 Experimental details

Exploring the nuclear structure of the heaviest $N = Z$ nuclei is a challenging job owing to the extremely low production cross-sections of these weakly-bound systems in fusion-evaporation reactions, which is the usual reaction mechanism employed for in-beam spectroscopy in this mass region. In order to overcome these difficulties, the recoil-$\beta$-tagging technique (RBT) [44] is employed, combining in-beam and decay spectroscopy methods, through requiring correlations with $\beta$-particles detected at the focal plane of a mass separator and using the fast decay characteristics of the super-allowed $\beta$-decay of the nucleus of interest to "tag" the in-beam $\gamma$ rays.

The experiment was performed at the Accelerator Laboratory of the University of Jyväskylä, where excited states in $^{94}$Ag were populated through the 1p3n fusion-evaporation channel induced by a $^{58}$Ni beam bombarding a 0.75 mg/cm$^2$ natural calcium target. The $^{58}$Ni beam was delivered by the K-130 cyclotron at four different beam energies ranging from 157 MeV to 183 MeV and intensities between 1 and 4 pnA (see Table 1). Prompt $\gamma$ rays were detected using the JUROGAM3 high purity germanium detector array, comprising 15 single-crystal detectors and 24 clover detectors housing 4 crystals each, all 39 detectors having BGO Compton-suppression shields [45]. The JYTube (Jyväskylä-York Tube) charged-particle detector, consisting of 96 plastic scintillator elements forming an hexagonal barrel, was placed surrounding the target to detect charged-particles evaporated from the fusion-evaporation products [46,47]. The MARA mass spectrometer was used to perform A/q identification of the recoils [46,48], positioning the mass slits and choosing the electric and magnetic field settings to maximise the transmission of A=94 fusion evaporation products to the focal plane detection system. At this point they were implanted in a double-sided silicon strip detector (DSSSD) after passing through a multiwire proportional chamber (MWPC). The DSSSD used in this work had a thickness of 300 μm and was segmented in 192 vertical and 72 horizontal strips on its front and back side, respectively. The MWPC provided position and energy loss information for the recoils thanks to a grid of 20 μm diameter gold-coated tungsten wires with 1 mm spacing in 3.5 mbar isobutane gas. A planar germanium detector was mounted immediately after the DSSSD to enable the detection of high-energy $\beta$-particles from subsequent radioactive decays after implantation. Events presenting signals in both the DSSSD and the MWPC in coincidence are assumed to be recoils while signals observed in the DSSSD alone come from decays.

All detector signals were time stamped by a global 100 MHz clock to allow temporal correlations to be made between $\gamma$ rays, charged-particles, recoils and subsequent radioactive decays. The data were analyzed with the GRAIN software package [49].

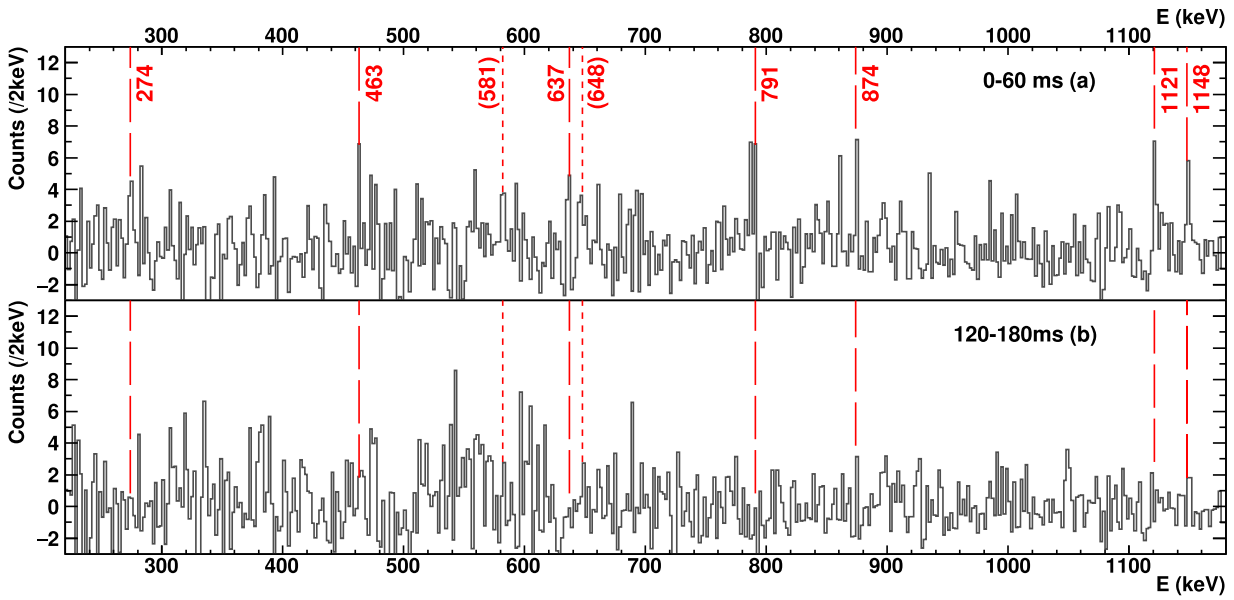


**Fig. 2** Background-subtracted, Doppler-corrected spectra for prompt $\gamma$ rays associated with $A = 94$ recoils observed in the focal plane decaying **a** within 60 ms or **b** between 120 and 180 ms from recoil implantation in coincidence with a high-energy $\beta$. Events in which two or more charged-particles were detected in the JYTube have been rejected. The background that has been subtracted is a total A = 94 spectrum (Fig. 1d), which represents a background due to false correlations between recoil and decay

## 3 Method and analysis

In order to maximize the statistics for the channel of interest, the excitation function was scanned by running at several beam energies (see Table 1). Following analysis of the data at the different beam energies, 167 MeV was selected as the optimum beam energy since $\gamma$ rays associated with fast $\beta$-decays with a lifetime similar to that of the known ground-state decay in $^{94}$Ag were observed to be strongest at this energy.

As expected, the analysis showed that the 1p3n fusion-evaporation channel, populating states in $^{94}$Ag, was very weak with multiple-charged-particle emission channels dominating the total fusion cross-section. As a result of the MARA spectrometer's ability to perform A/q selection, the strong competing reaction channels were predominantly constrained to $A = 94$ products: $^{94}$Pd, $^{94}$Rh and especially the 4p channel leading to $^{94}$Ru. Since they are all longer-lived nuclei than $^{94}$Ag (their half-lives are 9 s, 71 s and 51 min, respectively), requesting a high-energy $\beta$ associated with a fast decay, characteristic of the superallowed $\beta$-decay of the $T = 1$ ground-state of $^{94}$Ag), is expected to significantly suppress these competing channels.

Prompt, in-beam, $\gamma$ ray transitions in $^{94}$Ag were selected by requiring that they were recorded in coincidence with one or zero charged-particles detected in the JYTube and correlated with short-lived $A = 94$ recoils observed in the focal plane decaying through high-energy $\beta^+$ (>1.8 MeV, $Q \sim$13 MeV) particles. The resulting spectrum is shown in Fig. 1a, where we request a subsequent decay within 60ms, which corresponds to approximately two half-lives of the known lifetime of the $T = 1\ 0^+$ state, which is assumed to be the $^{94}$Ag ground-state. Comparison with $\gamma$ ray spectra recorded in combination with recoils with longer decay times, 120 to 180 ms (Fig. 1b), higher charged-particle multiplicity (Fig. 1c) and any A = 94 recoil (Fig. 1d) show that specific $\gamma$ rays, of energy 274(1), 463(1), 637(1), 791(1), 874(1), 1121(1) and 1148(1) keV, appear to grow with respect other $A = 94$ contaminants – see the marked transitions in Fig. 1a. A further two $\gamma$ rays are observed to be enhanced in Fig. 1a at 581(2) and 648(2) keV, however, these can only be given a very tentative assignment to $^{94}$Ag due to overlap with $\gamma$ rays with similar energies in $^{94}$Rh and $^{94}$Ru (a 582 keV transition from $15^-$ at 8854 keV in $^{94}$Ru, a 584 keV transitions from a second $15^-$ at 8737 keV in $^{94}$Ru and a 650 keV transition from $13^+$ at X+2547 keV in $^{94}$Rh).

The non-$^{94}$Ag $\gamma$ ray peaks (i.e. background contaminants) in Fig. 1a, have two principal origins. One source is false correlations between recoil and decay events, which will yield a background characteristic of the full, prompt, $A = 94$ $\gamma$ ray spectrum. The second source of background comes from true correlations where $\beta$-decays from longer-lived $A = 94$ recoils fall in the short (60 ms) time window and where some of the protons emitted in those reactions are missed by the JYTube. This is due to its imperfect detection efficiency, measured here to be 67% for the detection of a single proton,

which hampers the ability to reject the reaction channels with multiple protons emitted.

Most of the contaminating $\gamma$ ray peaks are identified as $^{94}$Ru transitions, corresponding to the 4p reaction channel, while evidence of $\gamma$ rays belonging to $^{94}$Rh, $^{94}$Tc and $^{90}$Mo (present due to the presence of an A/q ambiguity at the MARA focal plane) was also observed, as shown in Fig. 1d. Since false correlations appear to be a major source of background, it is possible to create background subtracted spectra by subtracting a background based on a total $A = 94$ gated spectrum. The background-subtracted spectrum for decays occurring within 60 ms of implantation, i.e. the background-subtracted version of Fig. 1a, is shown in Fig. 2a, where the same $\gamma$ ray transitions at 274(1), 463(1), 637(1), 791(1), 874(1), 1121(1), 1148(1) keV, along with the tentatively assigned 581(2) and 648(2) keV lines, are observed. The background-subtracted version of Fig. 1b, i.e. a spectrum gated between 120 and 180 ms, is shown in Fig. 2b, where the $\gamma$ rays in question appear to be very strongly suppressed. Thus, we conclude that the $\gamma$ rays listed above are associated with a $A = 94$ recoils decaying on the timescale of 10's of ms, which is consistent with the currently accepted value for the $^{94}$Ag $T = 1$ $0^+$ ground-state $\beta$-decay value (i.e., 27(2) ms [15,19]).

These $\gamma$ rays can therefore be associated with decays from, and between, states whose decay paths end at the short-lived $T = 1$ ground-state, and are not trapped by the low-lying $T = 0$ ($7^+$) isomer.

## 4 Discussion

The statistics were not sufficient to allow a $\gamma$-$\gamma$ coincidence analysis and hence it is not possible to determine the sequencing of the observed $\gamma$ rays. Based on a comparison with the $T = 1$ analog states in the even–even member of the $T = 1$ triplet, $^{94}$Pd, a possible scenario is that the 791, 874 and 637 keV $\gamma$ ray transitions may be very tentatively assigned as the analogs of the cascade of the 814, 905 and 659 keV E2 transitions de-exciting the $T = 1$ $6^+$ to the ground state in $^{94}$Pd. However, the possibility must also be considered that, in $^{94}$Ag, some of the even-$J$ $T = 1$ states do not decay by $\Delta T = 0$ stretched E2 transitions but instead through isovector $\Delta T = 1$ M1 transitions to low-lying $T = 0$ states. Such a pattern has been frequently observed in a number of odd–odd $N = Z$ cases [50–52].

In order to help understand what decay paths might be likely, we have performed shell-model calculations using the JUN45 interaction [43] in the $fpg$ model space. The Coulomb interaction has been added into the proton matrix elements, and single-particle energy levels were modified to account for Coulomb and magnetic monopole effects, following the prescription of reference [53]. The resulting wavefunctions have been analysed to examine electromagnetic transitions from the $T = 1$ states up to $6^+$ and all the $T = 0$ states that could potentially receive $\gamma$ ray feeding from those $T = 1$ states. In these calculations we have used effective charges of $\epsilon_p = 1.5$ and $\epsilon_n = 0.5$ and bare nucleon g-factors. Using the calculated level energies, we have then determined the relevant transition strengths, and produced a theoretical decay scheme based on the assumption that the first three $J > 0$ $T = 1$ states, and no others, are populated with equal intensity. In this way, we seek to predict the decay patterns of the $T = 1$ states, on the assumption that they are populated directly, as might be expected in a fusion evaporation reaction. The results are shown in Fig. 3a.

To test the appropriateness of this model for the $T = 1$ states in $^{94}$Ag, we have used the same model to predict the excitation energies of their $T = 1$ analog states in the even–even member of the triplet $^{94}$Pd. The predicted energies of the $J^\pi = 2^+, 4^+, 6^+$ states are 943, 1858 and 2500 keV, respectively. These compare favorably with the experimental values of 814, 1719 and 2378 keV [21,54], which gives confidence to the shell-model basis on which our predictions are made.

The predicted decay patterns of the populated $T = 1$ states, see Fig. 3a, suggest that the only E2 transition that might be observed is the $2^+ \rightarrow 0^+$ ($T = 1$) transition, with the other $T = 1$ states decaying by strong isovector M1 transitions to nearby $T = 0$ states. The $6^+ \rightarrow 4^+$ and $4^+ \rightarrow 2^+$ E2 transitions are highly suppressed. However, the veracity of these calculations relies on the assumption that the shell-model reproduces correctly the difference in absolute binding energies (and hence excitation energy) between the $T = 0$ states the $T = 1$ states. Our calculations show that if the $T = 0$ states are artificially raised by 500 keV, the E2 decay from the $T = 1$, $J^\pi = 4^+$ state begins to dominate over the isovector M1, and if they are instead raised by 750 keV, then the E2 decays will be the dominant paths from all three $T = 1$ states up to $6^+$. This latter scenario is demonstrated in Fig. 3b). However, it is important to stress that we do not have any experimental evidence for the separation of the $T = 0$ and $T = 1$ states, and so this is an illustrative exercise only. It is interesting to note that Xu et al. [6] have already demonstrated that the location of the $T = 0$ states, relative to the $T = 1$ states, is strongly dependent on the $np$ spin-aligned $g_{\frac{9}{2}}$ matrix element. Clearly, further work is required to determine the exact location of the $T = 0$ and $T = 1$ states in $^{94}$Ag.

From the predicted excitation energies of $^{94}$Ag in Fig. 3 and of $^{94}$Pd (see above) we can establish theoretical Coulomb energy differences (defined as $E_x(^{94}\text{Ag}) - E_x(^{94}\text{Pd})$. These are shown in Fig. 4. Most experimental, and theoretical, CEDs have a positive trend (e.g. [12,36], commonly explained in terms of the prevalence of $T = 1$ $np$ pairs in

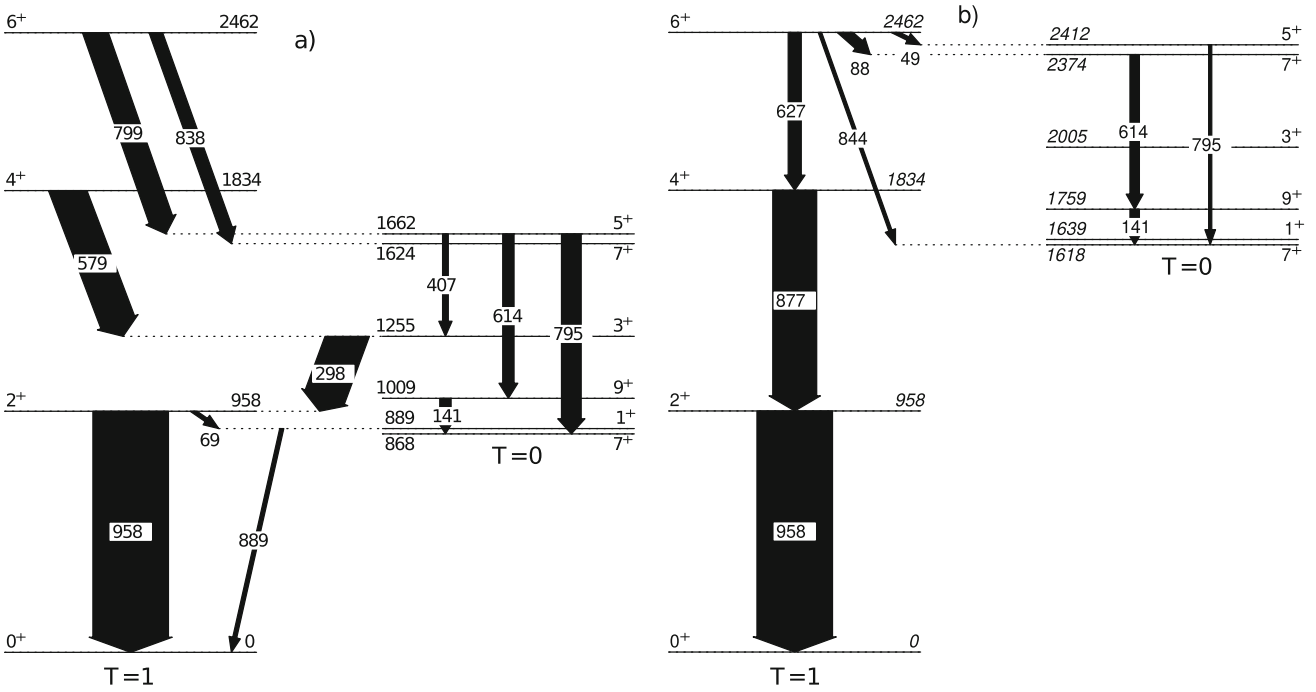


**Fig. 3** (Left) A theoretical $^{94}$Ag decay scheme, predicted by shell-model calculations assuming direct population of only the $2^+$, $4^+$ and $6^+$ $T = 1$ states. (Right) The predicted decay pattern when the $T = 0$ states are shifted upwards in energy by 750 keV. In both cases, only transitions with intensities higher than 4% are shown and states not involved in the de-excitation pattern are not depicted

the odd–odd $N = Z$ system, compared with $T = 1$ *nn* and *pp* pairs in the even–even neighbour – see e.g. [36] and references therein. Indeed, a negative CED trend has only been observed before for the mass 70 system $^{70}$Br-$^{70}$Se [24,51]. The green curve (triangles) in Fig. 4 shows the predicted shell-model calculation of the CED for $^{94}$Ag/$^{94}$Pd resulting only from the inclusion of the two-body Coulomb (multipole) interaction added into the proton matrix elements. This curve demonstrates the usual positive trend associated with angular-momentum re-coupling of the different types of $T = 1$ pairs among the triplet [36]. However, the red curve (circles) shows the effect of including in these CED calculation the single-particle monopole effects due to Coulomb and magnetic shifts in single-particle levels (labelled "lls", as is customary with this prescription [40]). In this case, the contribution of the single-particle shifts are dramatic, driving the predicted CED towards negative values for $J^\pi = 4^+, 6^+$.

Although we highlighted the possibility above that the 791, 874 and 637 keV transitions in $^{94}$Ag could be the analog transitions of the 814, 905 and 659 E2 transitions from the $6^+$ to the ground-state in $^{94}$Pd, we do not have sufficient evidence to make these assignments, and so the resulting experimental CED is not plotted in Fig. 4. However, our above shell-model analysis does indicate that we would expect to see the $2^+ \rightarrow 0^+$ transition among the $T = 1$ states of $^{94}$Ag. Since the typical magnitude of the CED for the $T = 1, 2^+$ state is a

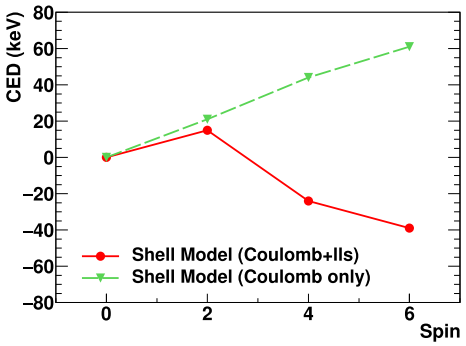


**Fig. 4** Theoretical Coulomb energy differences (CED) as function of $J$ between $T = 1$ levels in $^{94}$Ag and analog levels in $^{94}$Pd. Predictions with and without single-particle monopole effects are depicted in red circles and green triangles respectively

few 10's of keV, isospin symmetry arguments would suggest that the most likely candidate for the transition from this state is the 791-keV transition. This would yield a negative CED of -22 keV. This negative trend would be continued smoothly if the 874 and 637 keV transitions in $^{94}$Ag were assigned as the E2 decays of the $T = 1, 4^+$ and $6^+$ states, respectively. However, the shell-model analysis presented above suggests that it is not safe to give these assignments any confidence. We therefore present the current calculations as a prompt for future experimental work.

## 5 Summary

Nine prompt ( including two tentative) $\gamma$ ray transitions have been observed in this work that are associated with a short-lived $\beta$-decaying $A = 94$ nucleus produced via the 1p3n charged-particle evaporation channel and whose half-life is consistent with the currently accepted value for the $^{94}$Ag ground-state $\beta$-decay. Whilst spin and parity assignments of the decaying states have not been possible, the identified transitions can be assigned to $^{94}$Ag with a high level of confidence and are confirmed to be emitted in decay paths that lead to the $T = 1$, $J^{\pi} = 0^{+}$ ground-state. They represent the first observation of $\gamma$ rays from excited states in $^{94}$Ag. Possible correspondence between some of these transitions and the ones from analog states in $^{94}$Pd has been discussed. Shell-model calculations including multipole and monopole electromagnetic effects have been presented, and the results show that both intra-band transitions between the $T = 1$ states and isovector transitions between $T = 1$ and $T = 0$ states are possible, with intensities that strongly depend on the separation of the $T = 0$ and $T = 1$ states. Determining the relative position of the $T = 1$ states and the $T = 0$ states in this nucleus may provide insight into the strength of the $g_{\frac{9}{2}}\ np$ spin-aligned matrix element and hence further work is required to determine the detailed low-energy level scheme involving these observed transitions. A theoretical CED prediction up to $J^{\pi} = 6^{+}$ has been presented.

**Acknowledgements** The authors thank the GAMMAPOOL European Spectroscopy Resource for the loan of the detectors for the JUROGAM III array. Support has also been provided by the EU 7th framework programme, Project No. 262010 (ENSAR). We wish to acknowledge support from the UK STFC under Grants nos. ST/L005727/1, ST/P003885/1, ST/V001035/1, the Ministry of Science and ICT (Grant no. IBS-R031-D1). U. Forsberg would like to thank Birgit and Hellmuth Hertz' Foundation for financial support. C. Müller-Gatermann acknowledges the support of the U.S. Department of Energy, Office of Science, Office of Nuclear Physics, under contract number DE-AC02-06CH11357. J. G. Vega-Romero acknowledges CONACYT financial support.

**Data availability statement** The processed experimental data generated during the current study are available in the University of York Data Repository [55].



## References

1. W. Heisenberg, Uber den Bau der Atomkerne. I. Z. Phys. **77**, 1 (1932)
2. B. Cederwall, F.G. Moradi, T. Bäck et al., Evidence for a spin-aligned neutron-proton paired phase from the level structure of $^{92}$Pd. Nature **469**, 68–71 (2011)
3. B. Cederwall, X. Liu, O. Aktas et al., Isospin properties of nuclear pair correlations from the level structure of the self-conjugate nucleus $^{88}$Ru. Phys. Rev. Lett. **124**, 062501 (2020)
4. B.S.N. Singh, T.S. Brock, R. Wadsworth et al., Influence of the np interaction on the $\beta$ decay of $^{94}$Pd. Phys. Rev. C **86**, 041301(R) (2012)
5. G.J. Fu, J.J. Shen, Y.M. Zhao et al., Spin-aligned isoscalar pair correlation in $^{96}$Cd, $^{94}$Ag and $^{92}$Pd. Phys. Rev. C **87**, 044312 (2013)
6. Z.X. Xu, C. Qi, J. Blomqvist et al., Multistep shell model description of spin-aligned neutron-proton pair coupling. Nucl. Phys. A **877**, 51–58 (2012)
7. S. Zerguine, P.V. Isacker, Spin-aligned neutron-proton pairs in N $\sim$ Z nuclei. Phys. Rev. C **83**, 064314 (2011)
8. M. Aggarwal, Proton radioactivity at non-collective prolate shape in high spin state of $^{94}$Ag. Phys. Lett. B **693**, 489–493 (2010)
9. J. Cerny, D.M. Moltz, D.W. Lee et al., Reinvestigation of the Direct Two-Proton Decay of the Long-Lived Isomer $^{94}$Ag$^{m}$ (0.4 s and 6.7 MeV and (21 +)) . Phys. Rev. Lett. **103**, 152502 (2009)
10. M.L. Commara, K. Schmidt, H. Grawe et al., Beta decay of medium and high spin isomers in $^{94}$Ag. Nucl. Phys. A **708**, 167–180 (2002)
11. D.G. Jenkins, Reviewing the evidence for two-proton emission from the high-spin isomer in $^{94}$Ag. Phys. Rev. C **80**, 054303 (2009)
12. K. Kaneko, Y. Sun, T. Mizusaki et al., Isospin nonconserving interaction in the t = 1 analogue states of the mass-70 region. Phys. Rev. C **89**, 031302(R) (2014)
13. A. Kankainen, V.V. Elomaa, L. Batist et al., Mass measurements and implications for the energy of the high-spin isomer in $^{94}$Ag. Phys. Rev. Lett. **101**, 142503 (2008)
14. T. Kessler, I.D. Moore, H. Penttilä et al., Towards on-line production of N=Z $^{94}$Ag at IGISOL. Nucl. Instrum. Methods Phys. Res. B **266**, 4420–4424 (2008)
15. K. Moschner, A. Blazhev, N. Warr et al., Study of ground and excited state decays in N $\approx$ Z Ag nuclei. EPJ Web Conf. **93**, 01024 (2015)
16. I. Mukha, L. Batist, E. Roeckl et al., $\beta$-delayed proton decay of a high-spin isomer in $^{94}$Ag. Phys. Rev. C **70**, 044311 (2004)
17. I. Mukha, E. Roeckl, J. Döring et al., Observation of proton radioactivity of the (21$^{+}$) in high-spin isomer in $^{94}$Ag. Phys. Rev. Lett. **95**, 022501 (2005)
18. I. Mukha, E. Roeckl , H. Grawe et al., Comment on "reviewing the evidence for two-proton emission from the high-spin isomer in $^{94}$Ag". arXiv:1008.5346 [nucl-ex] (2009)
19. J. Park, R. Krücken, D. Lubos et al., New and comprehensive $\beta$- and $\beta$p-decay spectroscopy results in the vicinity of $^{100}$Sn. Phys. Rev. C **99**, 034313 (2019)
20. O.L. Pechenaya, C.J. Chiara, D.G. Sarantites et al., Level structure of $^{92}$Rh: implications for the two-proton decay of $^{94}$Ag$^{m}$. Phys. Rev. C **76** (2007)
21. C. Plettner, H. Grawe, I. Mukha et al., On the $\beta$-decaying (21$^{+}$) spin gap isomer in $^{94}$Ag. Nucl. Phys. A **733**, 20–36 (2004)
22. E. Roeckl, One-proton and two-proton radioactivity of the (21$^{+}$) isomer in $^{94}$Ag. Int. J. Mod. Phys. E **15**(2), 368–373 (2006)
23. K. Schmidt, T.W. Elze, R. Grzywacz et al., Decay properties of the new isotopes $^{94}$Ag and $^{95}$Ag. Z. Phys. A **350**, 99–100 (1994)
24. G. de Angelis, T. Martinez, A. Gadea et al., Coulomb energy differences between isobaric analogue states in $^{70}$Br and $^{70}$Se. Eur. Phys. J. A **12**, 51–55 (2001)

25. A. Boso, S.M. Lenzi, F. Recchia et al., Neutron skin effects in mirror energy differences: the case of $^{23}$Mg- $^{23}$Na. Phys. Rev. Lett. **121**, 032502 (2018)
26. A. Boso, S.A. Milne, M.A. Bentley et al., Isospin dependence of electromagnetic transition strengths among an isobaric triplet. Phys. Lett. B **797**, 134835 (2019)
27. J.R. Brown, M.A. Bentley, P. Adrich et al., First $\gamma$-ray spectroscopy of $^{49}$Fe and $^{53}$Ni: isospin-breaking effects at large proton excess. Phys. Rev. C **80**, 011306(R) (2009)
28. P.J. Davies, M.A. Bentley, T.W. Henry et al., Mirror energy differences at large isospin studied through direct two-nucleon knockout. Phys. Rev. Lett. **111**, 072501 (2013)
29. D.M. Debenham, M.A. Bentley, P.J. Davies et al., Spectroscopy of $^{70}$Kr and isospin symmetry in the T = 1 fpg shell nuclei. Phys. Rev. C **94**, 004300 (2016)
30. J. Henderson, D.G. Jenkins, K. Kaneko et al., Spectroscopy on the proton drip-line: probing the structure dependence of isospin nonconserving interactions. Phys. Rev. C **90**, 051303(R) (2014)
31. T.W. Henry, M.A. Bentley, R.M. Clark et al., Triplet energy differences and the low lying structure of $^{62}$Ga. Phys. Rev. C **92**, 024315 (2015)
32. K. Kaneko, T. Mizusaki, Y. Sun et al., Coulomb energy difference as a probe of isospin-symmetry breaking in the upper f p-shell nuclei. Phys. Rev. Lett. **109**, 092504 (2012)
33. R.D.O. Llewellyn, M.A. Bentley, R. Wadsworth et al., Spectroscopy of proton-rich $^{79}$Zr: mirror energy differences in the highly-deformed FPG shell. Phys. Lett. B **811**, 135873 (2020)
34. S.A. Milne, M.A. Bentley, E.C. Simpson et al., Isospin symmetry at high spin studied via nucleon knockout from isomeric states. Phys. Rev. Lett. **117**, 082502 (2016)
35. S.A. Milne, M.A. Bentley, E.C. Simpson et al., Mirrored one-nucleon knockout reactions to the $T_z = \pm\frac{3}{2}$ A=53 mirror nuclei. Phys. Rev. C **93**, 024318 (2016)
36. B.S. Nara Singh, A.N. Steer, D.G. Jenkins et al., Coulomb shifts and shape changes in the mass 70 region. Phys. Rev. C **75**, 061301(R) (2007)
37. P. Ruotsalainen, D.G. Jenkins, M.A. Bentley et al., Spectroscopy of proton-rich $^{66}$Se up to $J^\pi = 6^+$: Isospin-breaking effect in the A = 66 isobaric triplet. Phys. Rev. C **88**, 041308(R) (2013)
38. K. Wimmer, W. Korten, T. Arici et al., Shape coexistence and isospin symmetry in A = 70 nuclei: spectroscopy of the $T_z = -1$ nucleus $^{70}$Kr. Phys. Lett. B **785**, 441–446 (2018)
39. M.A. Bentley, Excited states in isobaric multiplets-experimental advances and the shell-model approach. Physics **4**(3), 995–1011 (2022)
40. M.A. Bentley, S.M. Lenzi, Coulomb energy differences between high-spin states in isobaric multiplets. Prog. Part. Nucl. Phys. **59**, 497–561 (2007)
41. M.A. Bentley, S.M. Lenzi, S.A. Simpson et al., Isospin-breaking interactions studied through mirror energy differences. Phys. Rev. C **92**, 024310 (2015)
42. S.M. Lenzi, M.A. Bentley, R. Lau et al., Isospin-symmetry breaking corrections for the description of triplet energy differences. Phys. Rev. C **98**, 054322 (2018)
43. M. Honma, T. Otsuka, T. Mizusaki et al., New effective interaction for $f_5pg_9$-shell nuclei. Phys. Rev. C **80**, 064323 (2009)
44. A.N. Steer, D.G. Jenkins, R. Glover et al., Recoil-beta tagging: a novel technique for studying proton-drip-line nuclei. Nucl. Inst. Methods Phys. Res. A **565**, 630–636 (2006)
45. J. Pakarinen, J. Ojala, P. Ruotsalainen et al., The jurogam 3 spectrometer. Eur. Phys. J. A **56**, 149 (2020)
46. J. Uusitalo, J. Sarén, J. Partanen et al., Mass analyzing recoil apparatus and MARA. Acta Phys. Pol. B **50**, 319 (2019)
47. W. Zhang, Experimental studies of neutron deficient nuclei in the A $\sim$ 110 and A $\sim$ 170 mass regions. PhD thesis, KTH Royal Institute of Technology Stockholm, Sweden, available at https://www.diva-portal.org/smash/get/diva2:1650608/FULLTEXT01.pdf (2022)
48. J. Sarén, The ion-optical design of the MARA recoil separator and absolute transmission measurements of the RITU gas-filled recoil separator. PhD thesis, University of Jyväskylä, available at https://jyx.jyu.fi/bitstream/handle/123456789/40107/978-951-39-4512-1.pdf?sequence=1&isAllowed=y (2011)
49. P. Rahkila, Grain-a java data analysis system for total data readout. Nucl. Instrum. Methods Phys. Res. A **595**, 637 (2008)
50. P. von Brentano, A.F. Lisetskiy, N. Pietralla et al., Isospin mixing in the $4^+$ doublet of $^{54}$Co. Eur. Phys. J. A **20**, 129–130 (2004)
51. D.G. Jenkins, N.S. Kelsall, C.J. Lister et al., T=0 and T=1 states in the odd-odd N=Z nucleus, $^{70}_{94}$Br$_{35}$. Phys. Rev. C **65**, 065307 (2002)
52. A.J. Nichols, R. Wadsworth, H. Iwasaki et al., Collectivity in A$\sim$70 nuclei studied via lifetime measurements in and $^{68,70}$Se. Phys. Rev. C **65**, 065307 (2002)
53. A.P. Zuker, S.M. Lenzi, G. Martínez-Pinedo et al., Isobaric multiplet Yrast energies and isospin nonconserving forces. Phys. Rev. Lett. **89**, 1–4 (2002)
54. N. Mărginean, D. Bucurescu, C.R. Alvarez et al., Yrast isomers in $^{95}$Ag, $^{95}$Pd and and $^{94}$Pd. Phys. Rev. C **67**, 061301R (2003)
55. https://doi.org/10.15124/c621e6eb-3212-49c6-8c1b-7431d1863dd4